BULLETIN OF THE EARTHQUAKE
RESEARCH INSTITUTE
Vol. 53 (1978), pp. 613-628

31. Summary of the Static and Dynamic Parameters of the Izu-Oshima-Kinkai Earthquake of January 14, 1978.

By Kunihiko SHIMAZAKI and Paul SOMERVILLE,

Earthquake Research Institute.

(Received Aug. 17, 1978)

The Izu-Oshima-Kinkai earthquake of Jan 14, 1978 involved right lateral strike slip motion together with a small dip slip component on a steeply northward dipping fault extending 17 km east of Inatori (see Fig. 1). The surface wave magnitude estimated from 47 component seismograms at 26 stations is 6.8.

The mainshock occurred approximately six seconds after a precursory event having approximately the same epicenter (Fig. 1 and Table 1). The hypocenter of the precursor, located by Tsumura (personal communication, 1978) is at a depth of approximately 10 km and is approximately 17 km east of Inatori. The relative location of the mainshock with respect to the precursor was determined using 11 teleseismic short-period seismograms and 17 Japanese low-gain seismograms on which the arrivals of both events could be identified (Fig. 2). The vertical short-period seismogram at ALQ (Fig. 3) provides supporting evidence for the hypocentral locations. The four phases are interpreted as the precursor P, the precursor pP 3 seconds later, the mainshock P arriving 7.5 seconds after the precursor P, and the mainshock pP arriving 1.5 seconds after the mainshock P.

Table 1. Origin time and hypocentral coordinates of the precursor and the mainshock

EVENT	TIME (JST)	LAT	LONG	DEPTH
Precursor	12 : 24 : 38.9	34°45′48″	139°14′04″	9.8
	±0.1 sec	±1.1 km	±0.8 km	±1.5 km
Mainshock	12 : 24 : 44.8	34°46′08″	139°12′24″	4.3
	±0.3 sec	±2.0 km	±1.8 km	±2.5 km
difference	5.9	2.2	3.6	5.5
	±0.3 sec	±1.6 km	±1.6 km	±2.0 km
	later	North	West	shallower

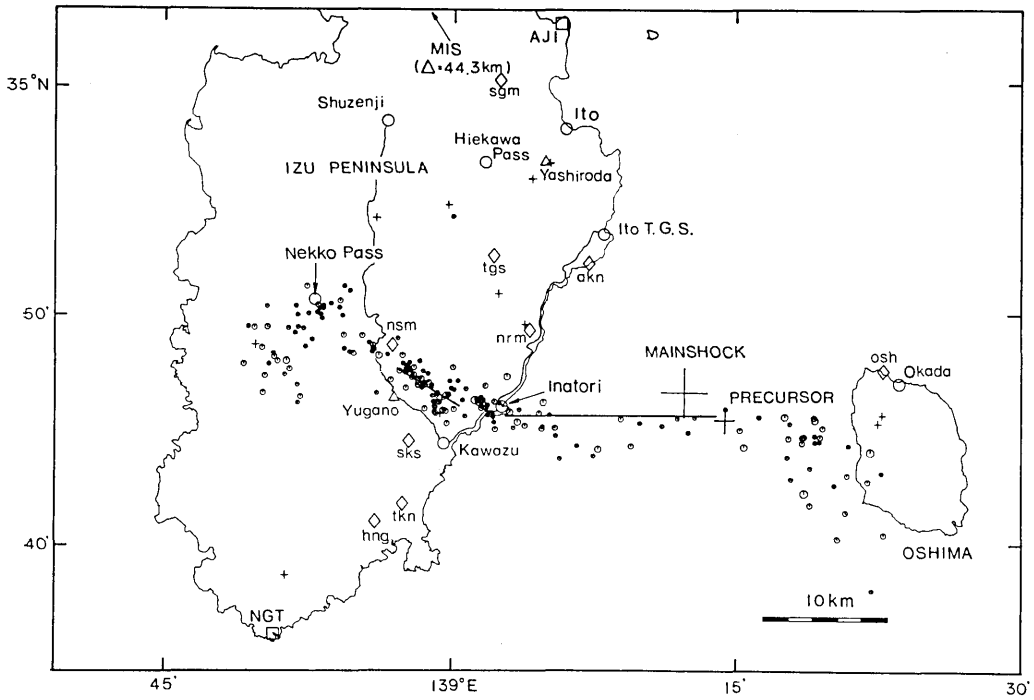

Fig. 1. Location of the mainshock relative to the precursor. The positions of the main and subsidiary faults are also shown. The open hexagons show aftershocks during Jan 19-31 whose magnitudes are greater than 1.4 (after TSUMURA et al., 1978). The small crosses indicate seismograph stations used to locate the aftershocks. The open squares indicate JMA stations whose strong motion seismograms are shown in Fig. 9. The open diamonds show distance measurement stations: hng, Hongo; nrm, Naramoto; nsm, Nashimoto; osh, Oshima lighthouse; sgm, Sugumoyama; sks, Sakasagawa; tgs, Togasano; tkn, Takaneyama. Two levelling routes from Ito Tide Gauge Station to Kawazu and from Shuzenji to Kawazu are also shown.

The mechanism solution of the mainshock was initially determined using S wave polarization angles because the precursor masked its long-period first motions. This solution was further constrained by SH waveforms and level changes along the east coast of the Izu Peninsula. Superposed on the mainshock solution (Fig. 4) are the P wave first motions of the precursor, which can be explained by the mainshock solution except at QUE. Therefore the P-wave first motions of the mainshock and the precursor should be the same except at stations near nodes such as QUE. This was used as a strong constraint in picking the P-wave arrival of the mainshock in the determination of its hypocenter as described above.

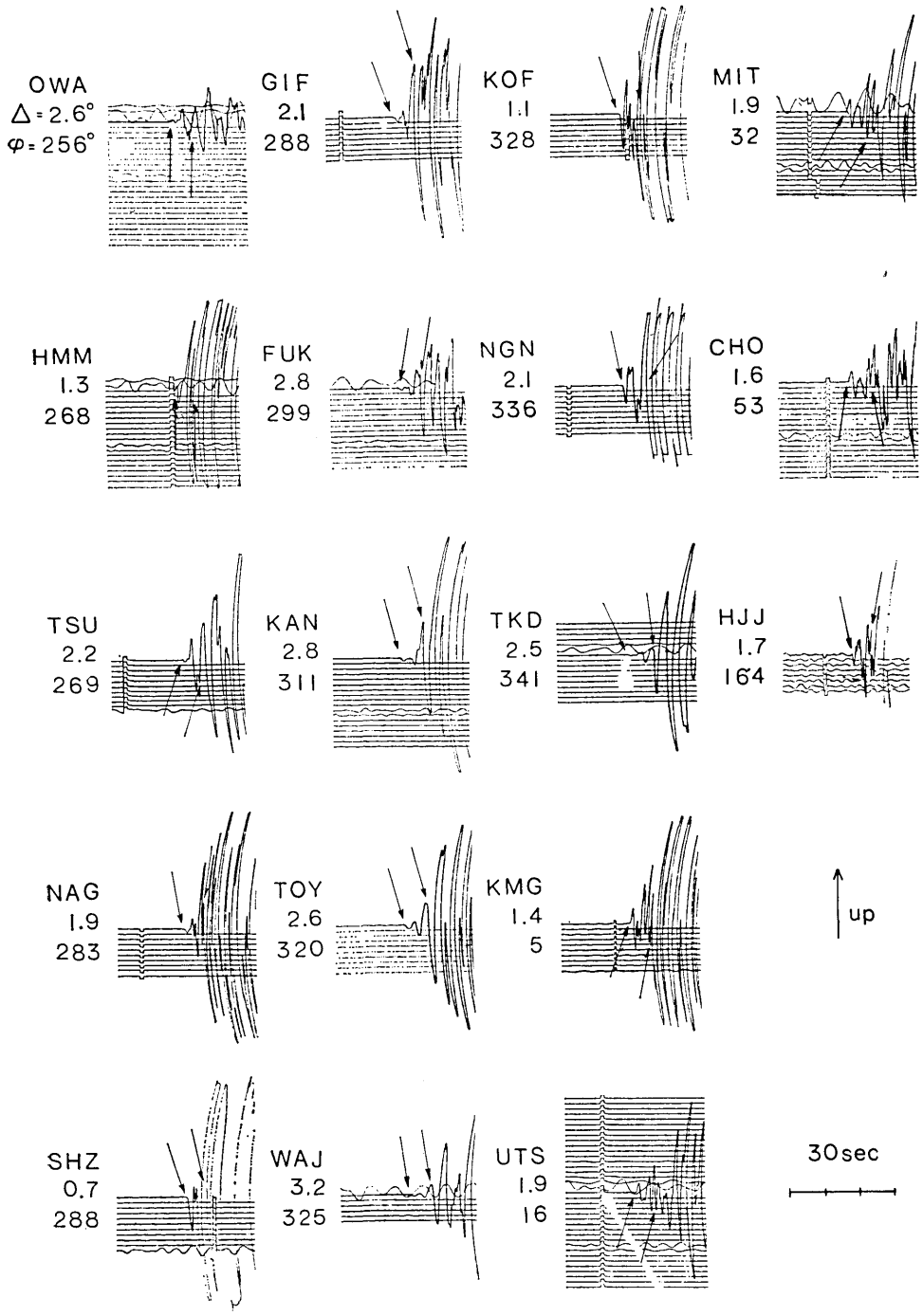

Fig. 2. JMA low-gain vertical seismograms. The two arrows in each seismogram indicate *P* arrivals of the precursor and the mainshock.

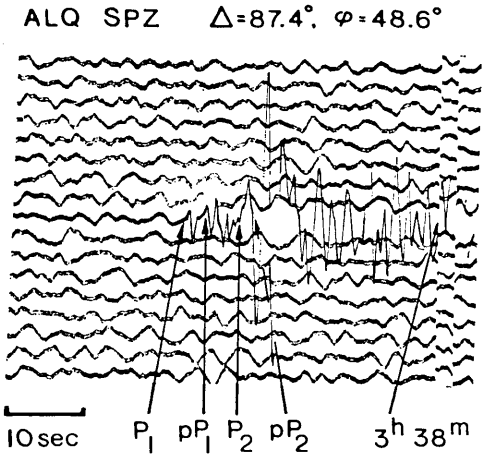

Fig. 3. Vertical short-period seismogram at ALQ (Albuquerque, New Mexico, USA) station.

The mechanism solution of the mainshock was closely constrained by SH waves at 13 WWSSN stations (Figs. 5 and 6). The strike, dip and slip angles were constrained within a few degrees of the values listed in Table 2. Levelling changes in the Izu Peninsula provided additional constraint on the slip angle, and also constrained the western end of the fault to lie just south of Inatori Peninsula (Figs. 7 and 12).

The mechanism solution is confirmed by the presence of clearly defined nodes in the radiation patterns of Love and Rayleigh waves (Fig. 8). The mean moment estimated from surface wave and SH wave amplitudes is 1.1×10^{26} dyne-cm. This is close to the value of $1.2-1.3\times10^{26}$ dyne-cm estimated independently from the observed distance change between Takaneyama in the Izu Peninsula and Oshima lighthouse, taking postseismic changes into account. Since these two observation points are diagonally opposite each other with respect to the fault (see Fig. 1), this moment estimate is stable and insensitive to fault length. Since the moment estimated

Table 2. Fault parameters of the Izu-Oshima-Kinkai earthquake of January 14, 1978

Surface wave magnitude	6.8
Seismic moment	1.1×10^{26} dyne-cm
Fault strike	N 90° W
Dip angle	85° North
Slip angle	188°
Fault length	17 km
Fault width	10 km
Depth	0—10 km
Dislocation: right lateral strike slip	183 cm
normal dip slip	26 cm
Rupture velocity	2.8 km/sec
Rise time	2 sec
Stress drop: infinite L/W ratio	41 bars
actual L/W ratio	65 bars
Dislocation velocity	93 cm/sec

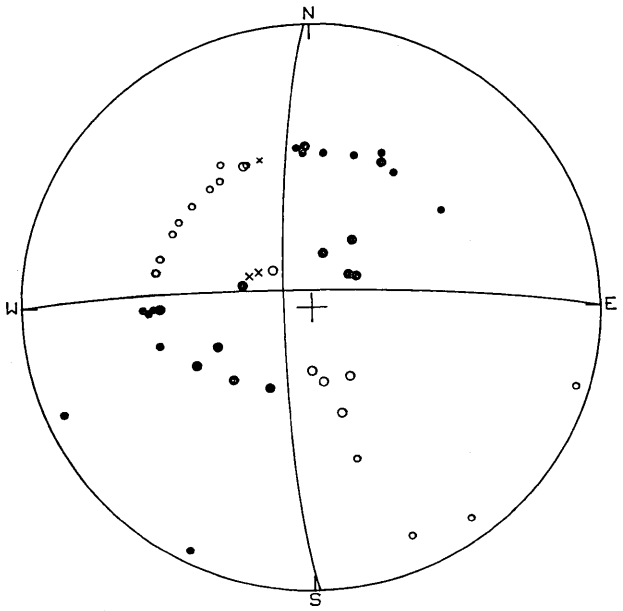

Fig. 4. Equal area projection of the fault plane solution for the main shock (lower hemisphere). The *P*-wave first motion data for the precursor are superposed. The solid circles represent compression first motions and the open circles represent rarefaction first motions. The crosses indicate arrivals with nodal character.

at 13-44 seconds from SH and surface waves is close to this static estimate, the faulting process inferred from the seismic waves probably represents the main process of faulting.

The SH waves provided constraints on the range of acceptable values of the ratio of fault length and rupture velocity. However the absolute values of fault length and rupture velocity remained unresolved, as did the rise time. These three parameters were determined using near field strong motion displacement seismograms at NGT, AJI and MIS which all lie within the range of direct first arrivals (Fig. 9). The rupture propagated westward at a velocity of 2.8 km/sec. The directivity effect is apparent on strong motion seismographs at other JMA stations with 180° azimuthal coverage on the northern side of the fault. The preferred fault length of 17 km agrees well with an independent estimate obtained from the positions of the two ends. The distances from Inatori Peninsula to the mainshock and precursor epicenters are 14 and 17 km respectively. The location of the fault corresponds to an E-W zone of aftershocks lying between Inatori and

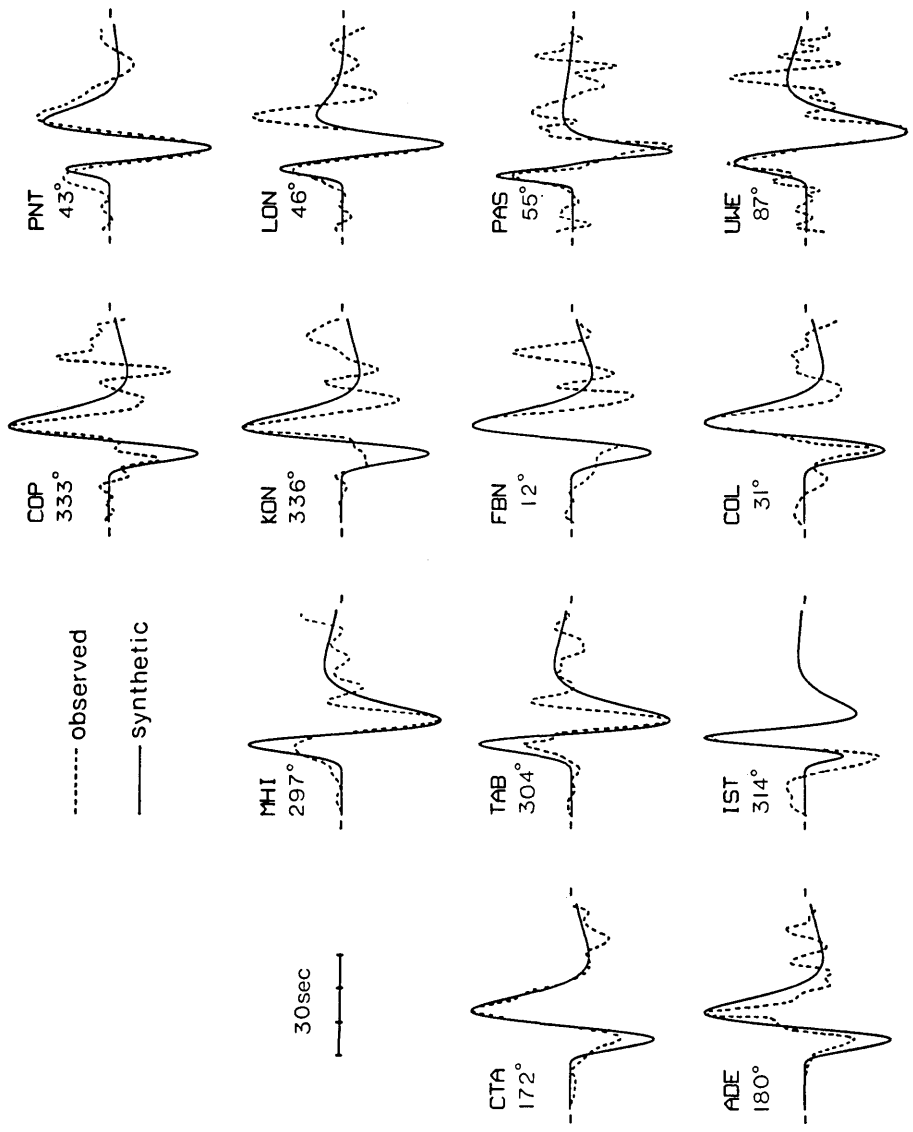

Fig. 5. Observed SH waveforms and matched synthetics. The numbers attached to each station code indicate station azimuths measured clockwise from north.

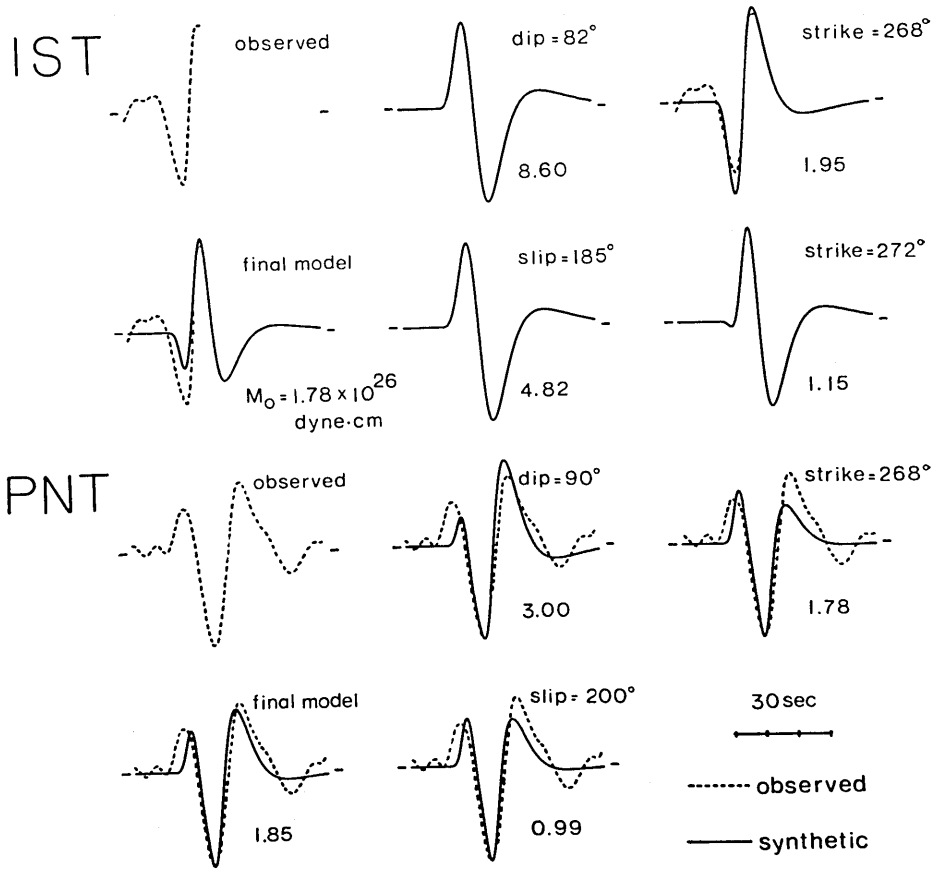

Fig. 6. Change of SH synthetic waveforms due to changes in various fault parameters.

Oshima (see Fig. 1) as shown by TSUMURA et al. (1978). For the preferred fault length of 17 km and an assumed fault width of 10 km estimated from the vertical extent of the aftershock zone (TSUMURA et al., 1978) we obtain an average displacement of 185 cm, comprised of 183 cm of right lateral strike slip and 26 cm of normal dip slip.

The tsunami source area estimated by HATORI (1978) from the arrival times of the tsunami coincides with the deformed area near the eastern end of the fault calculated from our model. AIDA (1978), using finite difference calculations, concluded that the best fault model has a length of 15 km with its eastern end 1.5 km west and 2 km south of the mainshock epicenter, and its western end a few kilometers west of Inatori.

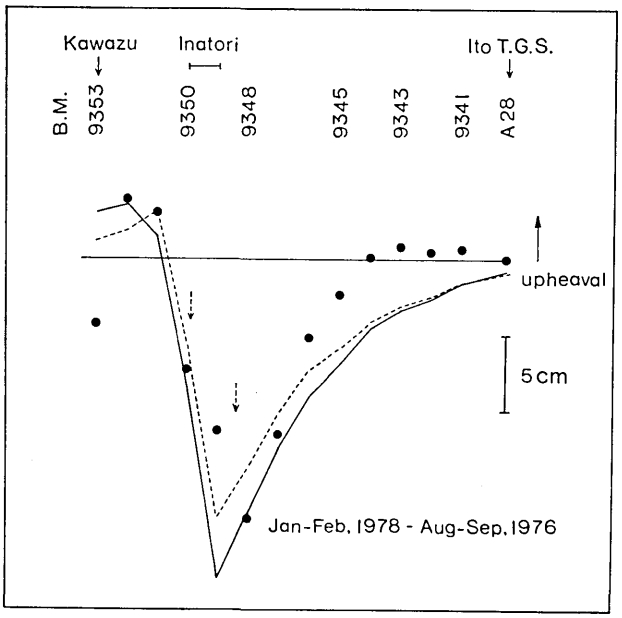

Fig. 7. Observed and calculated elevation changes along the east coast of the Izu Peninsula due to the Izu-Oshima earthquake. The levelling route is shown in Figs. 1 and 12. The solid circles show the observed elevation changes during the period from Aug-Sep, 1976 to Jan-Feb, 1978. It is assumed that bench mark A28 which is at Ito Tide Gauge Station 17 km northeast of Inatori did not move during the observation period. Bench mark 9350 is at the neck of Inatori Peninsula. The two arrows indicate the northern and southern boundaries of a block which co-seismically moved N 135°E. The solid line shows vertical displacements calculated from the main fault model. The dotted line includes the effect of subsidiary faulting.

Following the earthquake, a detailed survey of bottom topography between Oshima and the Izu Peninsula was conducted by the Hydrographic Department of the Maritime Safety Agency. It revealed a discontinuous system of approximately vertical E-W trending faults (HYDROGRAPHIC DEPARTMENT, MARITIME SAFETY AGENCY, 1978).

Surface faulting associated with the earthquake has been described by MURAI et al. (1978). It is limited to an area within a few kilometers of Inatori. TSUNEISHI et al. (1978) and YAMAZAKI et al. (1978) consider that the Omineyama fault is part of the fault plane of the earthquake and that the surface breakage along the Sengenyama fault is just a superficial phenomenon. However, it appears that block faulting occurred between the Omineyama and Sengenyama faults. The direction of motion of this block, N 135°E, is precisely the direction of strain north-

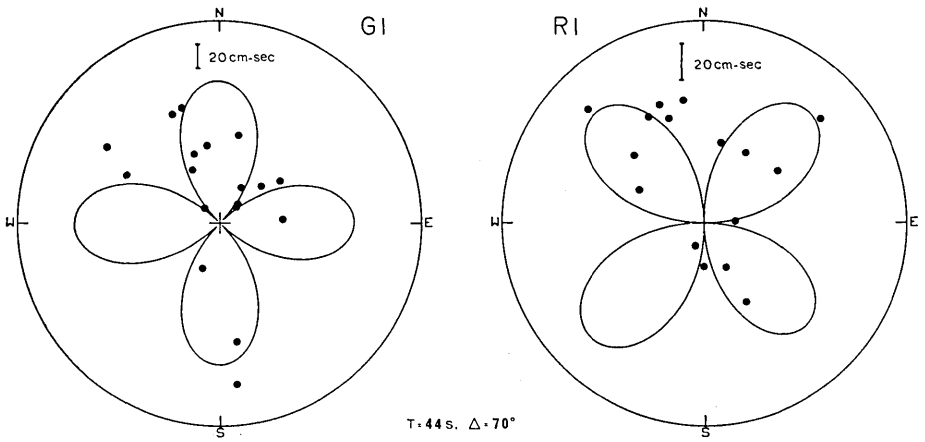

Fig. 8. Observed spectral amplitudes of Love (G1) and Rayleigh (R1) waves equalized to an epicentral distance of 70° on a standard WWSSN long-period seismograph (magnification=1500). Theoretical Love and Rayleigh wave spectral radiation patterns are superposed.

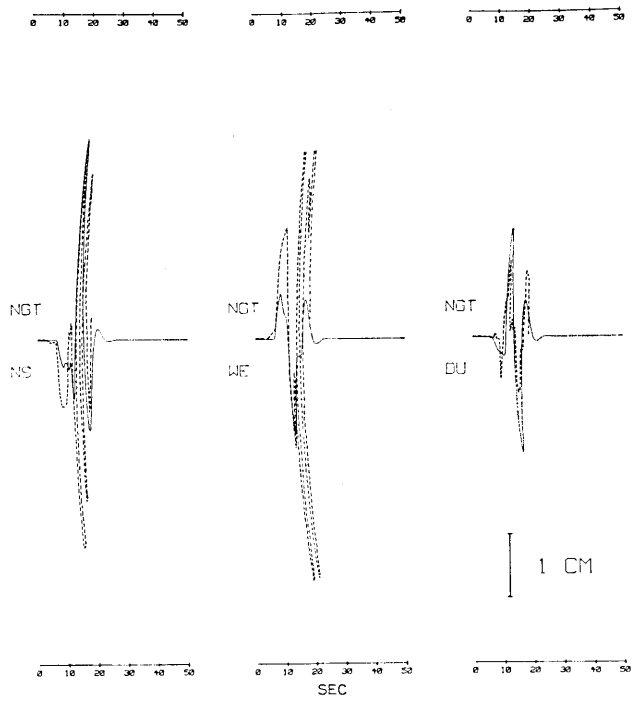

Fig. 9-1.

Fig. 9. Comparison of nearfield strong motion seismograms at Irozaki (NGT), Ajiro (AJI), and Mishima (MIS) with synthetic seismograms. The solid and dotted lines show the synthetic and observed seismograms, respectively.

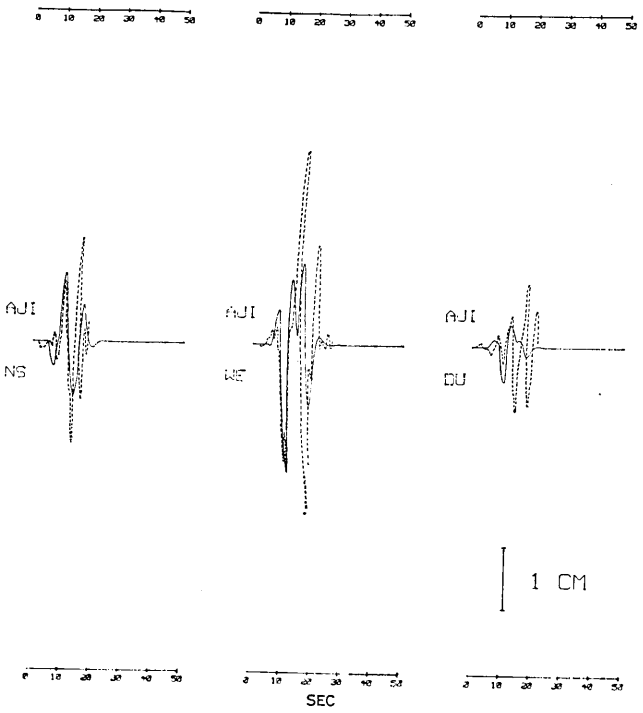

Fig. 9-2.

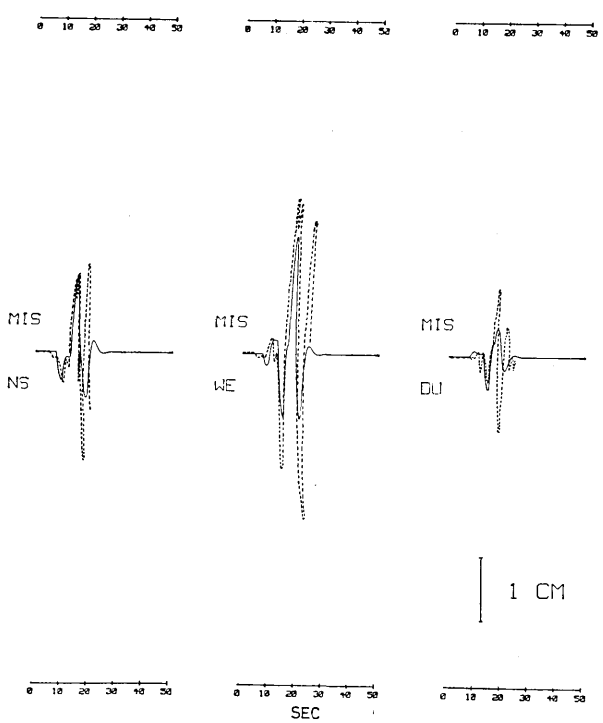

Fig. 9-3.

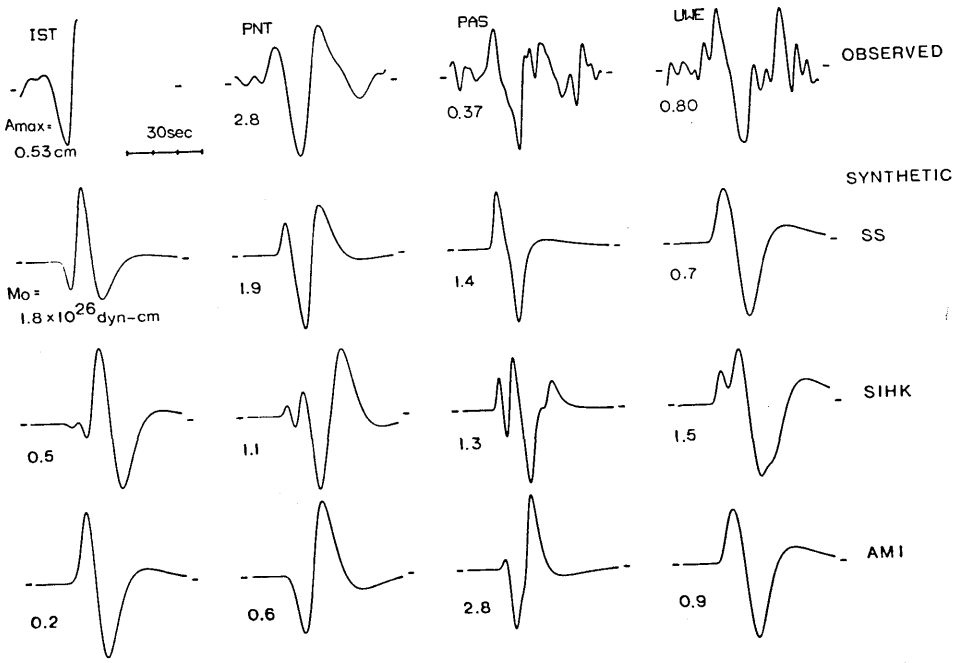

Fig. 10. Observed SH waveforms at Istanbul (IST), Turkey, Penticton (PNT), Canada, Pasadena (PAS), California, and Uwekahua (UWE), Hawaii, USA compared with synthetics calculated from the models of SHIMAZAKI and SOMERVILLE (SS), SUDO et al. (SIHK), and ANDO et al. (AMI). A_{max} denotes the maximum amplitude on the seismogram. The seismic moment M_o is obtained by matching the amplitudes of the observed and synthetic records.

west of the end of the fault expected from dislocation theory. Thus it appears that the existence of faults striking in this direction enabled the strain to occur in the form of faulting. If this faulting has been correctly interpreted, then the western end of the fault cannot lie inland, in agreement with the conclusion drawn from the levelling data along the eastern coast of the Izu Peninsula.

The distribution of destruction in the Izu Peninsula has been studied in detail by MURAI (1978). Widespread severe damage to houses was restricted to the vicinity of Inatori, and corresponded broadly with the location of surface breakage. The fact that the severity of destruction decreases progressively inland supports the conclusion that the mainshock did not propagate significantly inland.

The occurrence of strong aftershock activity in the Izu Peninsula has led many investigators to propose that the main faulting occurred inland. However, the absence of surface faulting inland tends to imply

Table 3. Observed and calculated changes in distance due to the Izu-Oshima-Kinkai earthquake of January 14, 1978

	PERIOD	OBSERVED	CALCULATED-1†	CALCULATED-2††
Oshima lighthouse-Sugumoyama	Dec 1977—Feb 1978	−5.2 cm	−4.2 cm	−4.4 cm
Oshima lighthouse-Togasano	〃	−8.6	−13.8	−14.6
Oshima lighthouse-Takaneyama	Dec 1977—Jan 1978	25.7	19.8	20.2
Naramoto-Akane	Sep 1976—Jan 1978	2.5	3.6	−1.1
Naramoto-Aogahira	〃	1.7	2.9	3.9
Naramoto-Seirigahara	〃	3.7	−0.6	−8.1
Naramoto-Chuchin	〃	20.0*	5.9	5.4
Sakasagawa-Nashimoto	Feb 1975—Feb 1978	−35.6 (−32.8#)	−4.1	−29.4
Sakasagawa-Hongo	〃	−1.1	1.2	3.3
Sakasagawa-Shirada	〃	40.2 (39.0#)	25.8	39.6
Shirada-Kazegoe	1975—Jan 1978	25.6	18.8	27.7
Shirada-Inatori	〃	2.8	−4.6	−1.7
Kazegoe-Inatori	1935—Jan 1978	106.0	82.3	92.8

* This value is probably affected by local land sliding at Chuchin (SHIIBANO, personal communication, 1978)

† Calculated changes in distance due to the main E—W trending fault.

†† The effect of the subsidiary fault is included. The assumed parameters of the subsidiary fault are: fault strike=N202°E, dip angle=75°NE, slip angle=182°, fault length=6.0 km, fault width=6.5 km, depth=0.5−7.0 km, right lateral strike slip =120 cm, normal dip slip=5 cm.

Corrected for the effect of the Kawazu earthquake of August 1976 by using the fault parameters obtained by Abe (1978).

(Geodetic data used in this study were provided by the Crustal Dynamics Department of the Geographical Survey Institute, Shizuoka University, and the Crustal Movements Survey Party of the Earthquake Research Institute.)

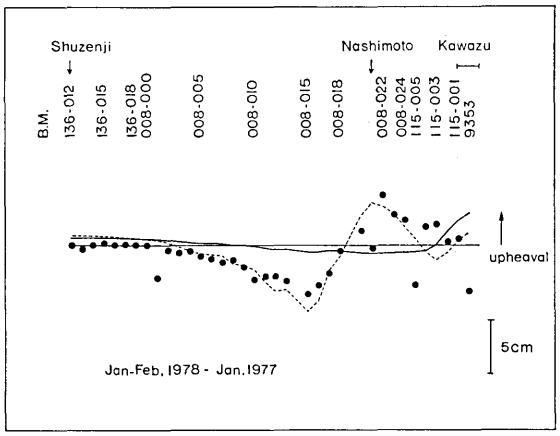

Fig. 11. Comparison of the observed elevation changes during the period from Jan, 1977 to Jan-Feb, 1978 with the calculated vertical displacements. The solid circles show the observed elevation changes. The levelling route is shown in Figs. 1 and 12. The solid line shows vertical displacements calculated from the main fault model. The dotted line includes the effect of subsidiary faulting.

the absence of main faulting because the two previous strike slip earthquakes in the Izu Peninsula having comparable magnitude (the 1930 North Izu and 1974 Izu-Hanto-Oki earthquakes) were both accompanied by surface faulting with displacements comparable to the seismologically determined dislocations.

In Fig. 10 we compare SH waveforms at critical stations calculated from the models of SUDO et al. (1978) and ANDO et al. (1978) with those of our model. The former two models, which both entail the main component of faulting inland, show considerable discrepancies with the observed seismograms. We conclude that it is unlikely that the main faulting propagated significantly inland.

However, we do not deny the possibility that some small subsidiary faulting occurred inland. Both levelling and distance change data indicate that a small amount of deformation occurred in an area near Nashimoto northwest of Inatori (Fig. 11 and Table 3). The data suggest a small right lateral strike slip fault segment trending roughly parallel to the aftershock zone between Inatori and Nekko Pass (see Fig. 12), whose length is only one-third of the length of the aftershock zone. The static moment of this assumed fault is about one order of magnitude smaller than that of the main fault. The fault parameters of the subsidiary fault cannot be tightly constrained because seismic data are

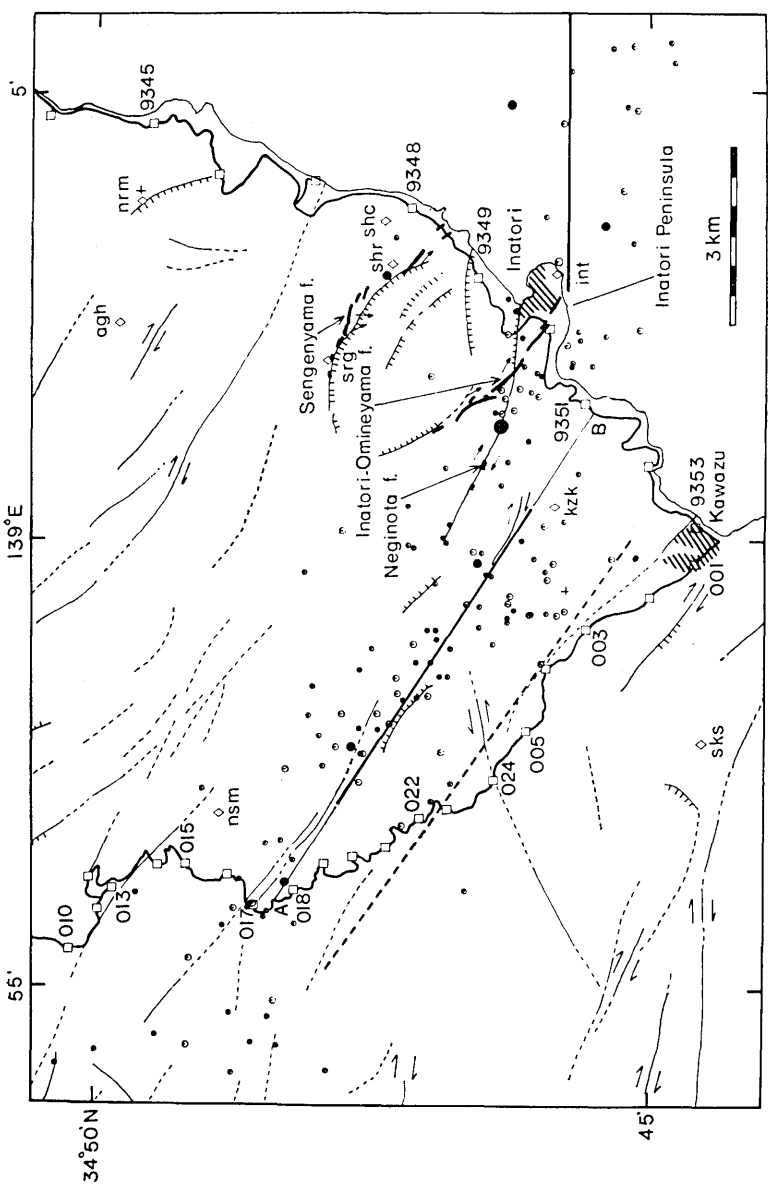

Fig. 12. Assumed subsidiary fault along the line AB and aftershock epicenters near and west of Inatori. The traces of surface faulting observed after the Izu-Oshima earthquake are shown by the thick lines (after MURAI et al., 1978). The attached arrows show representative relative motions. The main fault lies just south of Inatori Peninsula. The solid circles and open hexagons indicate epicenters of aftershocks during Jan 19-31 ($M \geqq 4.0$, large solid circle; $4.0 > M \geqq 3.0$, small solid circle; $3.0 > M \geqq 2.0$, large open hexagon; $2.0 > M \geqq 1.0$, small open hexagon; after TSUMURA et al., 1978). The small crosses show seismograph stations used to locate the aftershocks. The open squares indicate the locations of bench marks for the levelling survey. The open diamonds show distance measurement stations: agh, Aogahira; int, Inatori; kzk, Kazegoe; nrm, Naramoto; nsm, Nashimoto; shc, Chuchin; shr, Shirada; sks, Sakasagawa; srg, Seirigahara. The broken line indicates the position of the 1976 Kawazu earthquake fault (after ABE, 1978). Geologically active faults are also shown (after MURAI and KANEKO, 1976).

unavailable: we cannot recognise any distinct later phase corresponding to this faulting. In fact, this faulting may even have been aseismic. UMEDA and MURAKAMI (1978) suggest that the faulting motion was very slow on the basis of the small degree of damage to houses due directly to shaking.

This report is a revision of a preliminary one (SHIMAZAKI and SOMERVILLE, 1978a), and represents a summary of our paper (SHIMAZAKI and SOMERVILLE, 1978c) which will be published elsewhere. Preliminary reports of this study were presented at the 40th and 41st meetings of the Coordinating Committee for Earthquake Prediction (SHIMAZAKI and SOMERVILLE, 1978b).

Acknowledgments

We would like to thank the personnel of all the seismograph stations who were kind enough to send us seismograms. We also thank Barry RALEIGH, Dave HILL, Ken'ichiro YAMASHINA, Masahiro YAMAMOTO, Hiroo KANAMORI, and Prof. Daisuke SHIMOZURU for making various seismograms available to us.

References

ABE, K., 1978. Dislocations, source dimensions and stresses associated with earthquakes in the Izu Peninsula, Japan. *J. Phys. Earth* (in press).

AIDA, I., 1978. A numerical experiment for the tsunami accompanying the Izu-Oshima-Kinkai earthquake of 1978. *Bull. Earthq. Res. Inst.*, **53**, 863-873 (in Japanese).

ANDO, M., T. MIKUMO and Y. ISHIKAWA, 1978. Faulting process of the Izu-Oshima earthquake of January 14, 1978. *Programme and Abstracts, Seismol. Soc. Japan 1978*, No. 1, 63 (in Japanese).

HATORI, T., 1978. Tsunami source of the Izu-Oshima-Kinkai earthquake of 1978. *Bull. Earthq. Res. Inst.*, **53**, 855-861 (in Japanese).

HYDROGRAPHIC DEPARTMENT, MARITIME SAFETY AGENCY, 1978. Report to the Coordinating committee for Earthquake Prediction, 21 August 1978.

MURAI, I., 1978. Report to the Coordinating Committee for Earthquake Prediction, 20 February 1978.

MURAI, I. and S. KANEKO, 1976. Active fault map of the southern Kanto District. 14pp. Nagoya Univ. (Isao Matsuzawa), Nagoya, Japan.

MURAI, I., T. MATSUDA and K. NAKAMURA, 1978. Surface faults near Inatori associated with the 1978 Izu-Oshima earthquake. In Y. Osawa (editor), Earthq. Res. Inst., Tokyo Univ., "Research Report of the Coordinated Survey of Damage due to the 1978 Izu-Oshima Earthquake", 53-54 (in Japanese).

SHIMAZAKI, K. and P. SOMERVILLE, 1978a. Faulting mechanism of the Izu-Oshima earthquake of January 14, 1978. *ibid*, 11 (in Japanese)

SHIMAZAKI, K. and P. SOMERVILLE, 1978b. Summary of the fault parameters of the Izu-Oshima earthquake of January 14, 1978. *Rep. Coord. Comm. Earthq. Predict.*, **20**, 51-52 (in Japanese).

SHIMAZAKI, K. and P. SOMERVILLE, 1978c. Static and dynamic parameters of the Izu-Oshima, Japan, earthquake of January 14, 1978. Preprint.

SUDO, K., K. ISHIBASHI, N. HIRATA and I. KAWASAKI, 1978. Faulting process of the Izu-Oshima earthquake of January 14, 1978. *Programme and Abstracts, Seismol. Soc. Japan 1978*, No. 1, 60 (in Japanese).

TSUMURA, K., I. KARAKAMA, I. OGINO, M. TAKAHASIHI, K. KANJO and I. NAKAMURA, 1978. Foreshock and aftershock activity of the 1978 Izu-Oshima earthquake. *ibid*, 30 (in Japanese).

TSUNEISHI, Y., T. ITO and K. KANO, 1978. Surface faulting associated with the 1978 Izu-Oshima-Kinkai earthquake. *Bull. Earthq. Res. Inst.*, 53, 649-674.

UMEDA, Y. and H. MURAKAMI, 1978. Lineament of cracking of roads due to the Izu-Oshima earthquake and the area damaged by its largest aftershock. *Programme and Abstracts Seismol. Soc. Japan 1978*, No. 1, 22 (in Japanese).

YAMAZAKI, H., H. KOIDE and E. TSUKUDA, 1978. On the surface faults associated with the 1978 Izu-Oshima earthquake. *ibid*, 23 (in Japanese).

---

31. 1978年伊豆大島近海地震の静的および動的パラメター概報

地震研究所 島崎邦彦
Paul SOMERVILLE

1978年1月14日伊豆大島近海地震（表面波マグニチュード 6.8）は稲取より東へ 17 km 伸びた東西走向の右横ずれ断層によって生じた．断層面はほぼ垂直でやや北へと傾き，断層運動は小さな正断層成分をもっている．遠地短周期記象と気象庁の地震記象とから，主破壊は第一震の約6秒後に，ほぼ同じ場所で始ったと推定される．遠地ＳＨ波合成記象と観測記象との比較から主破壊は西へ伝播し，その伝播時間は6秒程度であることがわかる．さらに近地合成地震記象と気象庁強震計記象との比較から断層の長さは 17 km，断層上の変位の立ち上り時間は約2秒と推定される．表面波のスペクトル振幅とＳＨ波の振幅とから推定される地震モーメントの値は 1.1×10^{26} dyne-cm である．この値は伊豆半島の高根山と大島燈台との間の距離変化から，独立に推定される値，$1.2-1.3\times10^{26}$ dyne-cm にごく近く，地震波から推定される断層の動きは，主破壊のほぼ全容をとらえているものと思われる．測地データ，特に伊豆東岸の国土地理院水準測量成果から，この断層の西端は稲取岬の南，極めて近いところに達しているものと推定される．第一震，主破壊の開始点とこの西端との距離はそれぞれ，17 km，14 km で，震央位置の誤差を考えれば，先に述べた断層の長さと調和的である．地表にあらわれた断層は稲取より２～３km 以内までしか認められず，上記の断層位置の推定と調和的である．この主断層は，伊豆半島と大島との間に東西に伸びた余震分布に対応するものと思われる．水路部の調査では東西走向の短い断層が数本見い出されている．測地データのみは梨本付近に小さな副次断層の存在を示唆している。その走向は余震分布に平行で，右横ずれ断層であり，地震モーメントは主破壊の値より１桁オーダーが小さいものであろう．
